

This content has been downloaded from IOPscience. Please scroll down to see the full text.

Download details:

IP Address: 18.227.114.6

This content was downloaded on 24/04/2024 at 15:18

Please note that [terms and conditions apply](#).

You may also like:

[Measurement Possibilities of Thoracic \(C7-T12\) and Lumbar \(L1-L5\) Curvature](#)

S Surya, Dinesh Shanmugam and Murali Subramaniyam

[Innovation management based on proactive engagement of customers: A case study on LEGO Group. Part II: Challenge of engaging the digital customer](#)

S Avasilci and G Rusu

[Financial instruments for the development of the transport industry](#)

L Gerasimova

[SRP Meeting: Developments in Operational Health Physics, University of Birmingham, 25-26 March 1998](#)

An Introduction to Time-of-Flight Secondary Ion
Mass Spectrometry (ToF-SIMS) and its Application
to Materials Science

Sarah Fearn

Chapter 1

Introduction

For the last 50 years, secondary ion mass spectrometry (SIMS) has been at the forefront of high-resolution materials analysis and characterisation. A combination of factors makes SIMS unique amongst the analytical techniques widely available: it is able to measure all elements of the periodic table from H to U, along with isotopes and molecular species. Under optimum conditions the technique has extremely high sensitivity down to ppm (and in some cases ppb) coupled with very high surface specificity on the order of nm. This range of capabilities means that SIMS has been exploited in many wide-ranging areas of research and materials development. From its initial use as an instrument to investigate the material brought to Earth from the Moon missions of the 1960s, the application of SIMS can now be found in areas as diverse as conservation science to the development of renewable energy materials. In this introduction to time-of-flight secondary ion mass spectrometry (ToF-SIMS), an overall understanding of the main scientific principles underlying SIMS and its useful applications within the field of materials science will be given.

Over the years, SIMS instrumentation has dramatically changed since the earliest secondary ion mass spectrometers were first developed. Instruments were once dedicated to either the depth profiling of materials using high ion beam currents to analyse near surface to bulk regions of materials (dynamic SIMS), or time-of-flight instruments that produced complex mass spectra of the very outer-most surfaces of samples, using very low beam currents (static SIMS). Now, with the development of dual-beam instruments these two very distinct fields now overlap.

This book will highlight, in particular, the application of dual-beam ToF-SIMS for high-resolution surface analysis and characterisation of materials. Along with a brief overview of the underlying principles of the secondary ion mass spectrometry,

there will also be some examples of how dual-beam ToF-SIMS is used to investigate a range of materials systems and properties.

1.1 Overview

Time-of-flight secondary ion mass spectrometry (ToF-SIMS) is a mass spectrometry technique used to analyse the chemistry of materials, *in vacuo*. An energetic beam of primary ions (0.1–20 keV) is used to bombard a sample surface. The bombarding primary ion produces a variety of sputtered particles: monatomic and polyatomic particles of the sample are produced along with electrons and photons and re-sputtered primary ions. The secondary ions that are formed carry negative, positive and neutral charges. The desired secondary ions are extracted and detected using mass spectrometry. A schematic of the instrumental components of a dual-beam ToF-SIMS are shown in figure 1.1. In a dual-beam system a primary ion gun is used to generate the secondary ions to be analysed under static ion beam conditions (explained in more detail in section 3.1) for high-resolution surface mass spectrometry. The second ion beam (known as the sputter gun) can be used for the controlled erosion of the sample, known as sputter depth profiling. The removal of material in this controlled manner enables the composition from the surface to the bulk to be analysed.

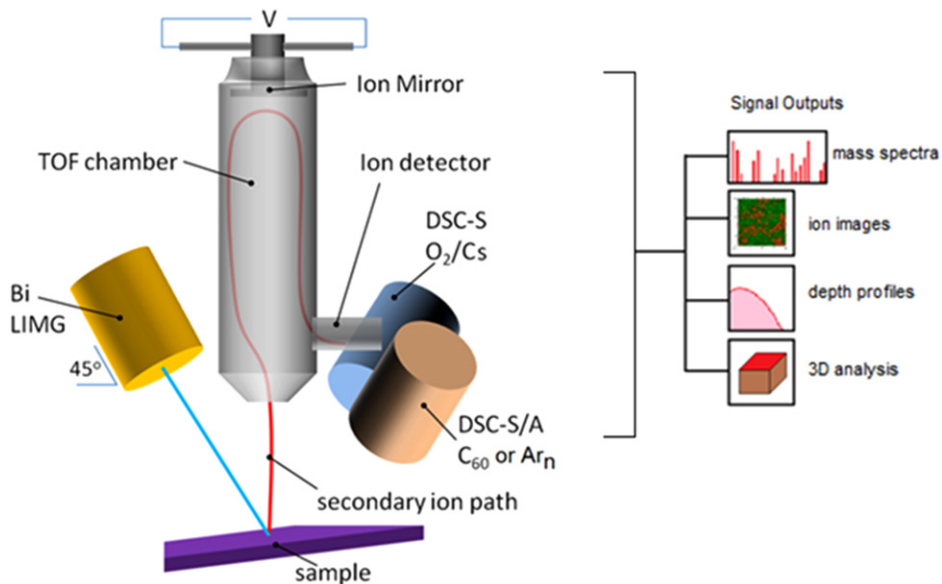


Figure 1.1. A schematic representation of the main components of a dual-beam time-of-flight secondary ion mass spectrometer. Secondary ions are sputtered from a target/sample by the primary ion gun. The sputtered secondary ions are extracted by an extraction potential into the flight tube and detected electronically, typically with a microchannel plate. Depending on the mode of operation of the instrument, a range of signal outputs can be obtained: mass spectra, ion images, depth profiles and 3D analyses.

1.2 Basic principles

Any atomic or molecular species that can be ionised and transported into a gas phase can be, in principle, analysed by mass spectrometry. At its basis secondary ion mass spectrometry, SIMS, is the measurement of the mass-to-charge ratio (m/z) of secondary ions generated from a target surface via ion beam bombardment. The formation of the secondary ions i.e. the ionisation, occurs at or very close to the emission of the particles from the surface. The ionisation process is, therefore, strongly influenced by the chemical state of the surface; this is known as the matrix effect. The ionisation and sputtering phenomena are complex processes, and a more in depth explanation of the mechanism can be found in the literature [1]. The emission of the secondary ions, however, can be described by the basic SIMS equation, shown below:

$$I_s^x = I_p C_x S \gamma F \quad (1.1)$$

where I_s^x is the secondary ion current of species x (i.e. the measured secondary ion counts of x), I_p is the primary ion beam current, C_x is the concentration of species x , S is the sputter ion yield of x and γ is the ionisation efficiency, i.e. the probability of the detected species forming positive or negative ions. Finally, F is the transmission of the analysis system.

The basic SIMS equation shows that the measured secondary ion counts, I_s^x , are directly proportional to the concentration, C_x , of the measured species, x , which implies that quantification can be easily made. However, as the measured secondary ion signal is also dependant on the chemical state of the surface where the ions have been emitted from, quantification is not so straightforward. The dependence of the ionisation of the measured species on the chemical state of the surface is, as previously stated, known as the matrix effect. This is a major hindrance to the quantification of many complex samples such as biological systems that have varying chemistry over the sample, and relevant standards are difficult to create. However, when standards can be accurately made, and the matrix is homogeneous as is the case for many silicon-based devices and semiconductors in general, quantification can be readily carried out with the use of implant standards. These are samples whereby a known ion implant of the element that is being measured is implanted to form a profile in the matrix material e.g. silicon.

The fundamental parameters of S , the sputter yield, and γ , the ionisation efficiency, are dependent on several factors relating to the selection of the ion beam and the properties of the target material. The sputter yield, S , is the amount of material removed during ion beam bombardment of the target. The sputtering yield is influenced, and increased, by the mass, charge and energy of the ion beam used. Put simply, a greater sputter yield will be obtained by a heavy bombarding ion beam species, as the energy is imparted closer to the sample surface. The properties of the target material, however, also influence the sputter yield and for any given ion beam energy the sputter yield for elements will vary by a factor of 3 to 5 over the periodic table, as shown by the early work by Wehner and co-workers [2]. An example of this

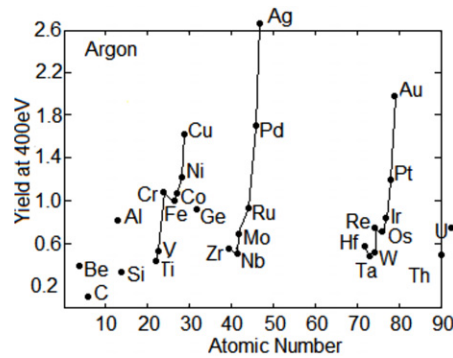


Figure 1.2. Sputtering yields for a 400 eV Ar ion energy for 28 elements versus the elements' atomic number. Reprinted from [2] with permission copyright 1961, AIP publishing LLC.

variation across the periodic table is shown in figure 1.2, whereby the yield variation due to Ar^+ ion beam sputtering was measured.

In covalent materials ion beam bombardment has a more damaging effect on the molecular and polymer structures and may rapidly destroy the chemical structure of interest. The amount of ion bombardment must therefore be limited to minimise the damage and another parameter is needed to monitor the sputtering. Along with the sputter ion yield, the disappearance cross-section, σ , is also monitored. The disappearance cross-section is an exponentially measured parameter and defined as the mean area damaged by one primary ion, and is related to the secondary ion intensity:

$$I_m = I_{m_0} \exp(-\sigma I_p) \quad (1.2)$$

where I_m is the recorded signal of the molecular species of interest, I_{m_0} is the original surface density of the respective molecular species, and I_p , the primary ion beam dose. Similarly to S , the disappearance cross-section also increases with the primary ion mass, energy and angle of incidence to the surface normal. The secondary ion efficiency, E , for a primary ion beam can thus be defined as:

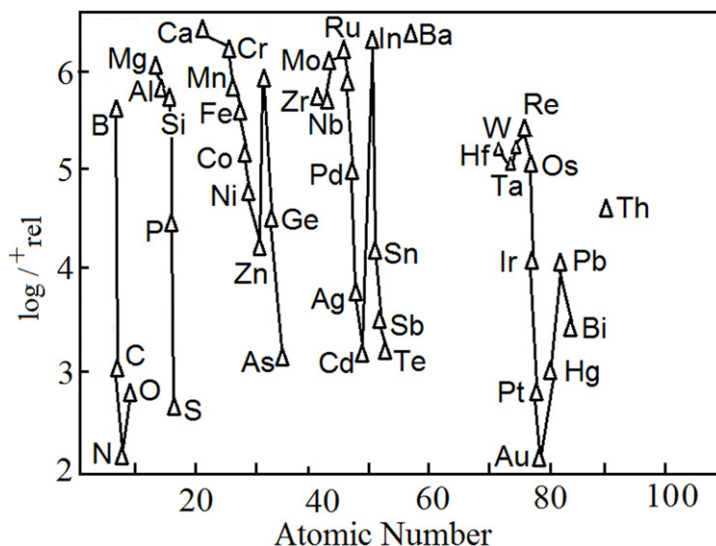
$$E = \frac{S}{\sigma}. \quad (1.3)$$

For optimised primary ion beam conditions both E and S should, therefore, be optimised and σ minimised. Generally, it has been observed from spin coated monolayer polymer samples that for the commonly available ion beams, efficiencies scale: $\text{Ga}^+ < \text{Au}^+$ or $\text{Bi}^+ < \text{Au}_3^+$ or $\text{Bi}_3^+ < \text{Bi}_2^{3+} < \text{C}_{60}^+$ [3]. Brunelle also assessed the sputtering parameters using the Bi ion source on biological tissue and the values are summarised in table 1.1 [4].

Ion yields from organic materials increase as the primary ion projectile is changed from an atomic species such as Ga^+ to a cluster ion source such as C_{60}^+ . This increase in ion yield is attributed to the way in which the cluster ion beam impacts upon the target surface. Upon impact, the cluster breaks up and the total energy of the ion

Table 1.1. Secondary ion yields, S , disappearance cross-section, σ , and ion bombardment efficiencies, E , for the bombardment of cholesterol in rat brain ($[M-H]^-$; m/z 385).

Primary ion	Energy (keV)	S (10^{-4})	σ (10^{-13}) (cm^2)	E (10^8) (cm^2)
Bi_1^+	25	0.836	2.75	3.04
Bi_3^+	25	7.06	4.14	17.1
Bi_3^{2+}	50	9.91	3.52	2.81

**Figure 1.3.** Variation of positive ion yield as a function of atomic number. Reprinted (adapted) from [5] with permission, copyright (1977) American Chemical Society.

beam is distributed over all of the atoms of the cluster, for example, a 20 KeV C_{60}^+ ion beam will result in an impact of only 666 eV per C atom. The penetration of the individual ion impacts results in less damage to the underlying structure of the sample, and a larger area of surface molecules are ejected from the surface. The erosion rate is also greatly increased so that any underlying damage is removed by the subsequent impacts. More recently the development of the Ar_n^+ ion cluster sources has dramatically improved the analyses of organic-based materials, and looks to surpass the use of C_{60}^+ ion beams. The development of ion beam sources and the effect on organic SIMS analyses will be discussed in more detail in section 2.2.

The ionisation efficiency, γ , is the ease or tendency of an element or molecule to form either a positive or negative secondary ion, and it is dependent on the ionisation energy or electron affinity respectively of the ion being measured. Elements in groups I and II of the periodic table have decreasing ionisation energies from the top to the bottom of the periodic table, and readily form positive ions: $\text{X} \Rightarrow \text{X}^+ + \text{e}$. Figure 1.3 highlights the variation of ionisation of the elements over the periodic table. Conversely, elements that have high electron affinities are

more likely to form negative ions. Such elements are situated on the far right hand side of the periodic table, for example, the halogens readily form negative ions with fluorine being the most reactive.

References

- [1] Sigmund P 1969 *Phys. Rev.* **184** 383
- [2] Laegreid N and Wehner G K 1961 *J. Appl. Phys.* **32** 365
- [3] Vickerman J C and Briggs D (ed) 2013 *ToF-SIMS: Materials Analysis by Mass Spectrometry* (Chichester: IM)
- [4] Brunelle A, Touboul D and Laprevote O 2005 *J. Mass Spectrom.* **40** 985–99
- [5] Storms H A, Brown K F and Stein J D 1977 *Anal. Chem.* **49** 2023